



Poisson's ratio of high-performance concrete

Bertil Persson*

Lund Institute of Technology, Division of Building Materials, Lund University, P.O. Box 118, SE-221 00 Lund, Sweden

Received 21 October 1998; accepted 6 July 1999

Abstract

This article outlines an experimental and numerical study on Poisson's ratio of high-performance concrete subjected to air or sealed curing. Eight qualities of concrete (about 100 cylinders and 900 cubes) were studied, both young and in the mature state. The concretes contained between 5 and 10% silica fume, and two concretes in addition contained air-entrainment. Parallel studies of strength and internal relative humidity were carried out. The results indicate that Poisson's ratio of high-performance concrete is slightly smaller than that of normal-strength concrete. Analyses of the influence of maturity, type of aggregate, and moisture on Poisson's ratio are also presented. The project was carried out from 1991 to 1998. © 1999 Elsevier Science Ltd. All rights reserved.

Keywords: Creep; Elastic moduli; Long-term performance; Mechanical properties; High-performance concrete

1. Introduction

At low stress (up to 60% of the compressive strength) the elastic strain in normal-strength concrete (NSC) is followed in parallel by lateral strain of a magnitude varying between 0.15 and 0.20. At high stress, microcracking starts to develop parallel to the direction of the stress. Because of this microcracking the transverse strain increases at higher stress. Close to the ultimate strength, Poisson's ratio increases rapidly until failure occurs. The transverse expansion increases the compliance (i.e., the unit-stress deformation, ϵ/σ) of NSC during creep. The lateral strain also affects the size of the elastic modulus. Taking Poisson's ratio, ν , into account, this modulus will be reduced by ν^2 .

$$\nu = \frac{\epsilon_{\text{lat}}}{\epsilon_{\text{ax}}} \quad (1)$$

where ν denotes Poisson's ratio, ϵ_{ax} denotes the axial deformation of the specimen, and ϵ_{lat} denotes the lateral strain of the specimen during the creep test.

Few reports exist regarding Poisson's ratio of high-performance concrete (HPC). Brooks [1] and Brooks and Hynes [2] studied Poisson's ratio for Compresit, formally known as compact-reinforced composite (CRC), reported by Bache [3]. The calculations were based on experiments on plain HPC with a strength of 159 MPa and an elastic modulus of 58 GPa, and on fiber-reinforced CRC with a compressive strength of 195 MPa and an elastic modulus of

62 GPa. The water/cement ratio of the HPC was 0.22. The silica fume content was 24% calculated on the basis of the cement content. Poisson's ratio ($\nu = 0.19$ for the plain HPC and $\nu = 0.22$ for reinforced HPC) was calculated. In the present work a similar HPC was studied, therefore the results of the previous studies mentioned above are of great interest.

2. Methods

2.1. Material and preparation of specimens

Chemical composition and characteristics of the cement are stated in Table 1 [4]. The characteristics of the aggregates are given in Table 2 [5]. The mix compositions are shown in Table 3 [4]. A condition for good workability was a linear-logarithmic grading curve of the particles in the fresh HPC. Table 4 shows the number of studied specimen (1,002 in all). All the cylinders were 0.055 m in diameter and 0.30 m long. The sealed specimens were covered with 2-mm butyl rubber. The 100-mm cubes for studies of strength and relative humidity (RH) were prepared in the same way. The measurement equipment was connected to steel items cast in the cylinders, as seen in Fig. 1. The ambient climate was held at 20°C and 55% RH.

2.2. Methods

2.2.1. Conditions

Both air-cured and sealed HPCs were studied. Thermocouples continuously registered the internal temperature of

* Corresponding author. Tel.: +46-46-222-4591; fax: +46-46-222-4227.

E-mail address: bertil.persson@byggttek.lth.se

Table 1
Chemical composition of the cement (%) [4]

CaO	SiO ₂	Al ₂ O ₃	Fe ₂ O ₃	MgO	K ₂ O	Na ₂ O	SO ₃	Specific surface (Blaine)	Density
64.9	22.2	3.36	4.78	0.91	0.56	0.04	2.00	302 m ² /g	3220 kg/m ³

Table 2
Characteristics of the aggregates [4,5]

Material/characteristics	Elastic modulus (GPa)	Compressive strength (MPa)	Split tensile strength (Mpa)	Ignition losses (%)
Quartzite sandstone, Hardeberga	60	330	15	0.3
Granite, Norrköping	61	150	10	1.7
Crushed sand, Bålsta	59	230	14	2

the specimen. The internal temperature varied between 19 and 21°C. Dew-point meters performed the test of RH after calibration according to ASTM E 104-85 [6]. At commencement of testing the age of the HPC was either 1 or 2 days (stress/cube strength = 0.6) or 2 or 28 days (stress/cube strength = 0.3). The ambient RH was held at 55% RH.

Table 3
Mix proportions and main characteristics of the HPCs (kg/m³ dry material) [4]

Material	Mix number								
	1	1(3)	2	3	4	5	6	7	8
Quartzite (8–11 mm)	460	440							
Quartzite (11–16 mm)	460	440	965	910		1010	985		1065
Sand, Åstorp (0–8 mm)	800	780	820	790		750	755		690
Granite, Norrköping (11–16 mm)								1030	
Gravel, Toresta (8–16 mm)					1095				
Natural sand, Bålsta (0–8 mm)					780			780	
Cement, Degerhamn Std.	430	410	440	445	455	495	530	490	545
Granulated silica fume	21	21	44	45		50	51		55
Silica fume slurry					23			49	
Air-entraining agent	0.02	0.04		0.02					
Superplasticizer	2.6	2.8	4.5	3.8	5.1	4.6	7.6	8.6	10.8
Water/cement ratio	0.38	0.38	0.37	0.37	0.33	0.31	0.30	0.30	0.25
Air content (% by volume)	4.8	7.0	1.1	4.0	0.9	1.1	1.2	1.0	1.3
Aggregate content	0.74	0.74	0.73	0.72	0.75	0.71	0.70	0.72	0.70
Aggregate/cement ratio	4	4	4.1	3.8	4.1	3.6	3.3	3.7	3.2
Density (kg/m ³)	2,335	2,245	2,440	2,360	2,510	2,465	2,480	2,500	2,490
Slump (mm)	140	140	160	170	45	200	130	45	45
28-day drying strength (MPa)	69	50	85	69	89	99	106	112	114
1-year drying strength (MPa)	70	54	89	76	97	109	112	121	125
3-year drying strength (MPa)	69		91		97		115	121	127
28-day sealed strength (MPa)	89	62	105	95	101	121	126	122	129
1-year sealed strength (MPa)	101	65	117	98	115	129	145	131	154
2-year sealed strength (MPa)	112				115			131	
3-year sealed strength (MPa)			123	102			141		145
4-year sealed strength (MPa)	102				113			129	

Compressive strength observed for 100-mm cube.

2.2.2. Loading and optimizing the MTS (Material Testing System, Minneapolis, MN, USA) machine

The lateral strain as well as the axial strains was studied during 66-h short-term creep tests (Fig. 1). The lateral strain was measured at one point and the axial strains were observed on three sides of the specimen. Data on the strain were collected rapidly during the loading and unloading procedure. Data were collected over the first 2 s of load duration to obtain the Poisson's ratio. The lateral and axial strains were also observed during the unloading of the short-term testing. Two Poisson's ratios, ν , were thus obtained for each mix composition of HPC and each age (Table 3), one at loading and one at unloading after 66 h of creep. Normally the measured value of ν stabilized within 0.4 s at loading and 0.7 s from unloading [7,8]. To avoid dynamic effects on the ν , the calculation of ν was performed for measurements at 1.5 s after loading and 1.8 s after unloading (the time being limited).

Before the creep tests were started, the strength was obtained on cubes from the same batch of HPC as the cylinders. The strength from the same batch of HPC was also recorded when the HPC was 28 days old (Table 3). The capacity of the MTS machine was enhanced to a sufficient level. As a preparation for the loading procedure, an extra, identically prepared specimen was placed in the MTS machine. The loading rate was 1800 MPa/s. A special routine was used:

Table 4
Estimated number of specimens

Type of specimen	Cube 100 mm	Cylinder Ø55 mm
Basic creep (short-term)		38
Compressive strength	900	32
Drying creep (short-term)		32
Internal relative humidity	900 ^a	32 ^a
Quasi-instantaneous loading		70 ^b

^a The same specimen was used for strength studies.

^b Specimens from short-term studies.

- The position of the specimen was measured in the MTS machine to ensure that it was correct.
- A 0.1-kN loading and an oscillation of ~ 1 Hz was applied to the extra cylinder specimen.
- The gain, loading speed, and braking rate of the loading in the MTS machine were set.
- The loading in the MTS machine was recorded.
- Linear variable differential transformers (LVDTs) recorded the deformation of the cylinder specimen in a computer.
- Both the loading and the deformations were plotted to ensure that no overload existed.
- A short analysis was performed of the pretest before the final loading was done.

2.2.3. Start of testing

To begin testing, several steps were followed:

- The LVDTs were firmly connected to steel items cast in the cylinder (Fig. 1).
- The position of the cylinder in the MTS machine was adjusted to avoid eccentricities.
- A 0.1-kN loading was applied to the cylinder specimen to avoid dynamic effects at loading.

- An ambient climate box was placed and a constant climate provided by air conditioning for half an hour before the quasi-instantaneous loading was started.
- Thermostability between the specimen and the ambient climate was established.
- The ambient RH was set at $RH = 55\%$.
- The computer recording of the LVDT deformations was started.
- The loading was applied in the MTS machine within 1 s from starting the computer recorder.
- About 6,000 measurements were recorded during 3 s.
- The loading was applied within 0.015 s without any overload at the start of the testing.

2.2.4. Unloading

The hydraulic conditions in the MTS machine (i.e., the size of the pipes and the servo-controlled accumulator) required an unloading period of about 1 s. The unloading procedure was not done quasi-instantaneous, as was the loading. After a time of recovery specimens of all HPCs except type 2 were used for repeated quasi-instantaneous loading and unloading at 3-min intervals.

3. Results and accuracy

Influence on Poisson's ratio, ν , of the type of the type of aggregate was observed. Fig. 2 shows ν at loading and unloading of drying HPC vs. the relative 28-day strength at loading and unloading. The calibration was performed to obtain an accuracy of ± 0.002 mm. However, the measurement accuracy of the LVDTs was within a displacement of ± 0.0005 mm. Poisson's ratio was evaluated according to Eq. (1). The natural logarithm was calculated as shown in Eq. (2):

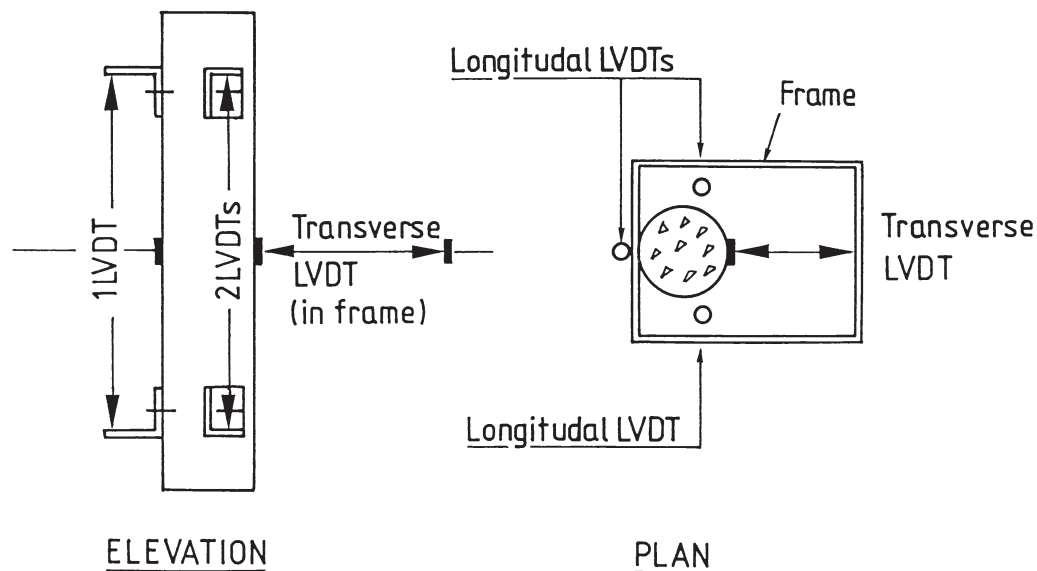


Fig. 1. Experimental setup for studies of Poisson's ratio.

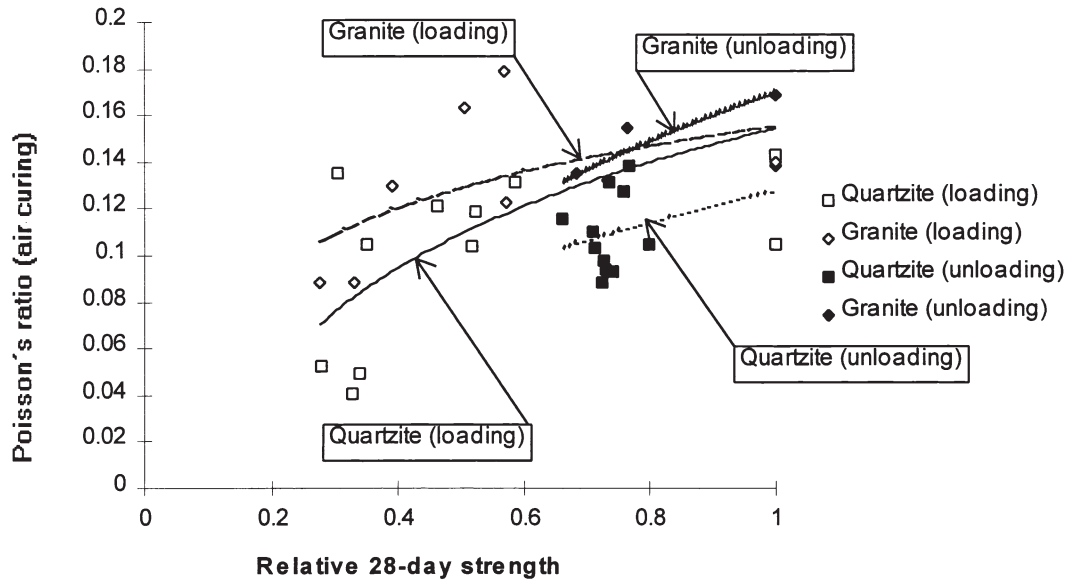


Fig. 2. Poisson's ratio of air-cured HPC vs. the relative 28-day strength. Aggregate type is given.

$$\ln v = \ln \epsilon_{lat} - \ln \epsilon_{ax} \quad (2)$$

After differentiation the maximum relative error, $\delta v/v$, was obtained ($\delta \ln v / \delta v = 1/v$) [see Eq. (3)]:

$$\delta v/v = \delta \epsilon_{lat} / \epsilon_{lat} - \delta \epsilon_{ax} / \epsilon_{ax} \quad (3)$$

For a young HPC (type 3) the relative error $\delta v/v \sim 0.17$ was obtained, which was a fairly large relative error. For a mature HPC (type 1) the relative error $\delta v/v \sim 0.11$ was obtained, which also was a fairly large relative error.

The reason for the large error may be the small measured distance: only 55.5 mm. Since the calculated accuracy was low, the real accuracy was studied by means of 48 supplementary experiments on mature HPC (Table 3). Table 5 gives the HPC properties of the study on long-term Poisson's ratio. Fig. 3 shows the long-term Poisson's ratio obtained. The coefficient of variation was small (Fig. 4), normally less than 0.04. The effect of type of the type of aggregate on Poisson's ratio was confirmed.

A small amount of eccentricity could not be avoided. The longitudinal strain was measured at three points but the transverse strain at only one point, which made it possible to calculate the longitudinal eccentricity. However, Daerga

and Elfgrén [9] have shown that eccentricities most often occur in HPC during both compression and tension. Bending in the cylinder may also affect the lateral dimensions. The size of the effect of the bending could not be estimated since only one LVDT was utilized. The measurement device was placed within the climate box in the MTS machine. However, to avoid any possible temperature effects on the measurement frame, only very short-term lateral displacements of the cylinder were calculated (within a 2-s period). It was possible also to study the incremental Poisson's ratio. Because of possible effects of small alterations of the temperature, this possibility was not utilized.

4. Analysis and discussion

4.1. Air curing

Fig. 4 shows different accuracy parameters such as the standard deviation, average, and variation coefficient of Poisson's ratio, v . The results were observed on repeated tests on air-cured HPCs given in Table 3. As shown in Fig. 4, v exhibited coefficients of variations generally less than 0.04, which is acceptable. From Fig. 2 a tendency of Poisson's ratio at loading or unloading of drying HPC, v_D , was correlated to the relative 28-day strength, as seen in Eq. (4):

$$v_D = k_D \cdot [0.05 \cdot \ln(f_c/f_{c28}) + 0.13] \quad (0.2 < f_c/f_{c28} < 1) \quad (4)$$

where f_c denotes the compressive strength of HPC at loading or unloading (MPa); f_{c28} denotes the compressive strength of the HPC at 28 days (MPa); \ln denotes the natural logarithm; $k_D = 1.2$ for HPC with granite (mixes 4 and 7), $k_D = 1$ otherwise; D denotes air curing (drying in RH = 55%); and v_D denotes Poisson's ratio at loading or unloading of drying HPC.

Table 5
Properties of HPCs of the study on long-term Poisson's ratio.

HPC mix	Age (days)	Stress, σ (MPa)	Strength, f_c (MPa)	f_c at 28-day age, f_{c28} (MPa)	σ/f_c	f_c/f_{c28}
1	550	20.7	68	69	0.30	0.99
2	540	25.8	89	86	0.29	1.03
3	510	27	69	58	0.39	1.19
4	720	26.6	101	91	0.26	1.11
5	450	38.7	116	106	0.33	1.09
6	380	33.3	116	111	0.29	0.96
7	580	34.9	121	117	0.29	1.03
8	400	35.4	129	118	0.27	1.09

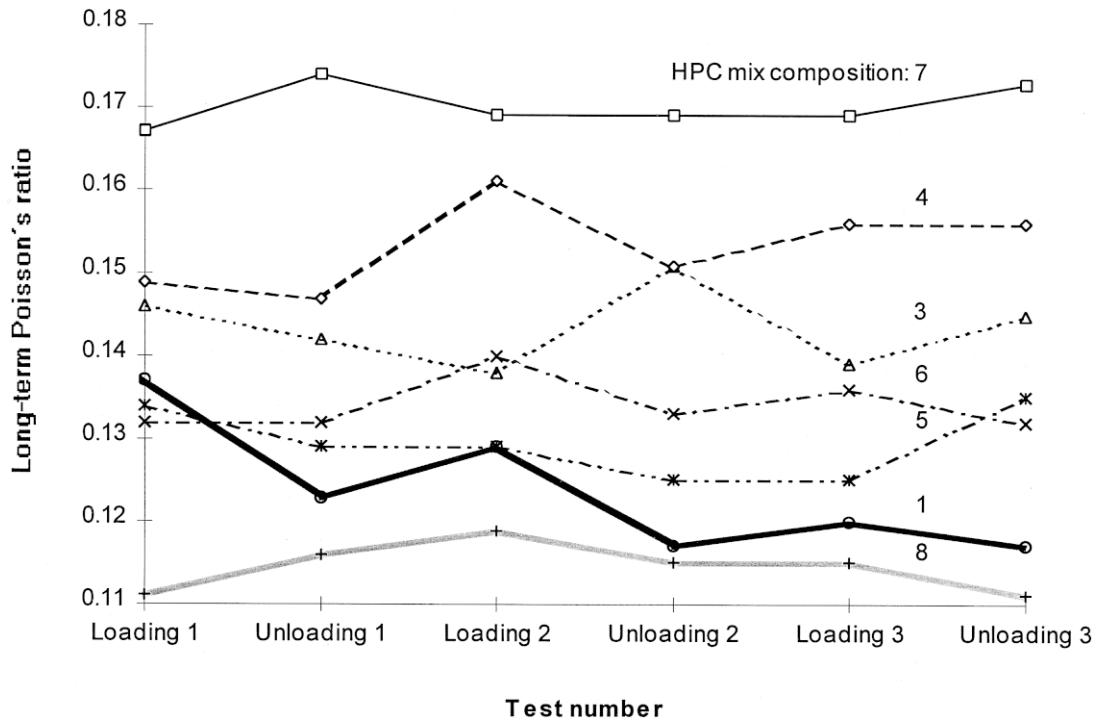


Fig. 3. Long-term Poisson's ratio. Type of HPC mix is given in Table 3.

4.2. Sealed curing

Fig. 5 shows Poisson's ratio, ν , on HPC with sealed curing obtained from exactly the same type of experiments as the ones with air curing [7,8]. Like the results for air-cured

specimens, ν for sealed HPC with granite is slightly larger than for HPC with quartzite. The reason for this difference is unknown. Maybe the higher strength of quartzite as compared to granite (more than twice as large compressive strength and 50% larger split tensile strength) influences ν .

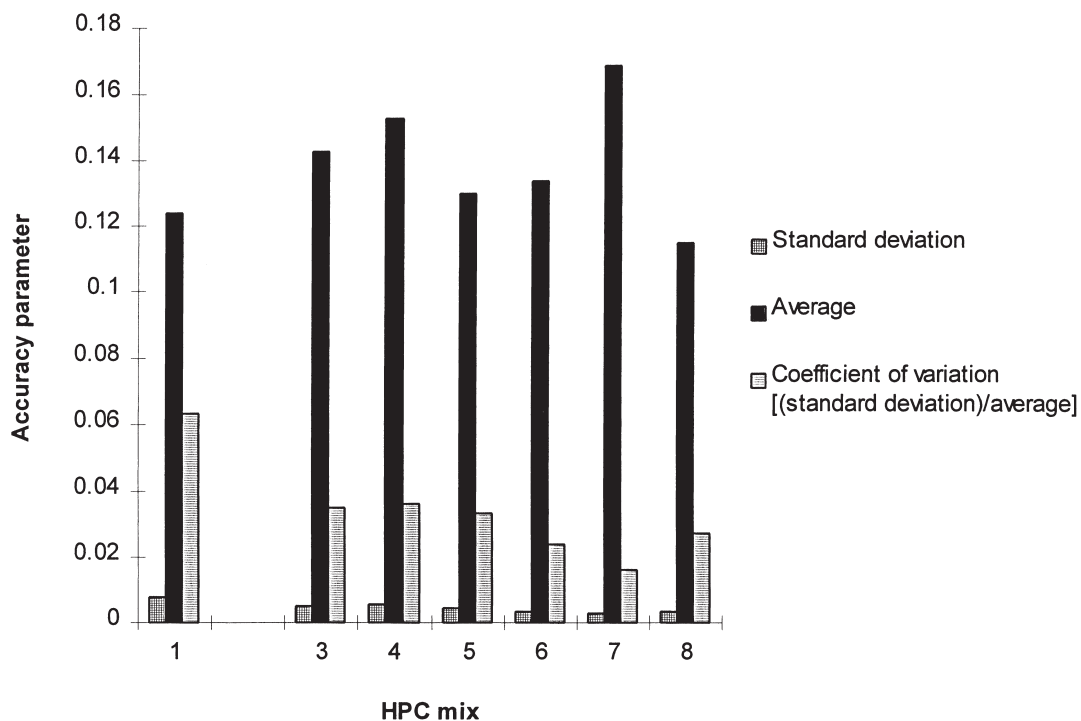


Fig. 4. Standard deviation, average, and variation coefficient of Poisson's ratio of air-cured HPC.

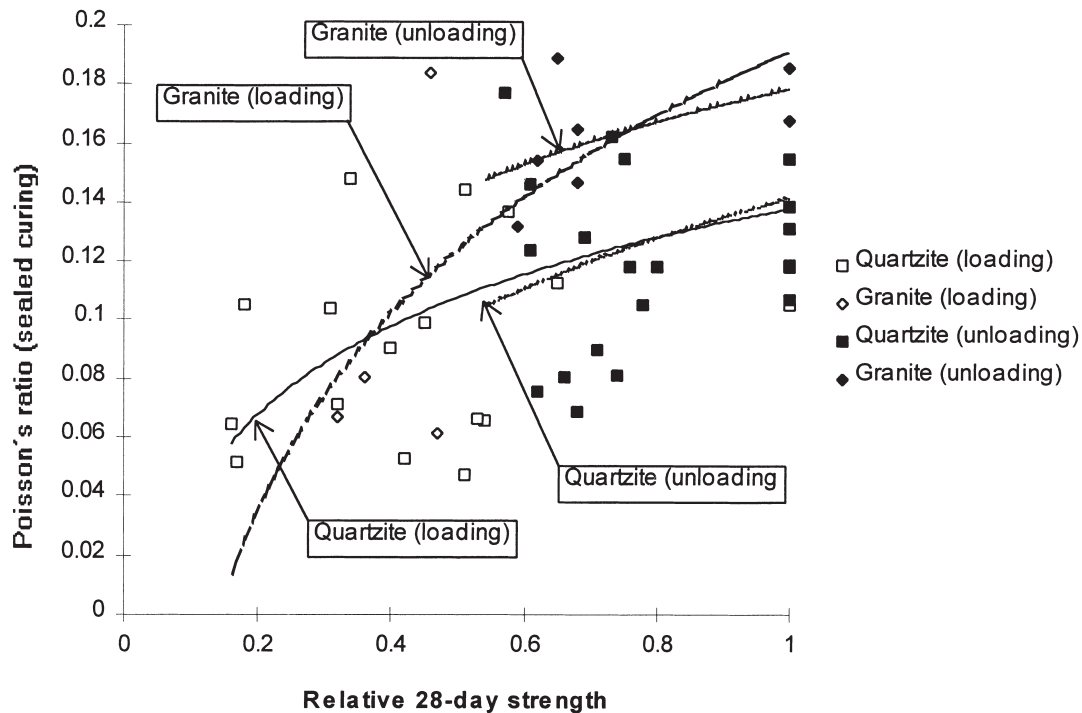


Fig. 5. Poisson's ratio of sealed HPC vs. the relative 28-day strength. Aggregate type is given.

From Fig. 5, a tendency of Poisson's ratio at loading or unloading of sealed HPC, ν_B , was correlated to the relative 28-day strength [see Eq. (5)]:

$$\nu_B = k_B \cdot [0.04 \cdot \ln(f_c/f_{c28}) + 0.14] \quad (0.2 < f_c/f_{c28} < 1) \quad (5)$$

where f_c denotes the compressive strength of HPC at loading or unloading (MPa); f_{c28} denotes the compressive strength of the HPC at 28 days (MPa); \ln denotes the natural logarithm; $k_B = 1.4$ for HPC with granite (mixes 4 and 7), $k_B = 1$ otherwise; B denotes sealed curing (based on studies of basic creep); and ν_B denotes Poisson's ratio at loading or unloading of sealed HPC.

4.3. Effect of aggregate and moisture

The observed long-term Poisson's ratio was about 30% larger for HPC of mix 4 or 7 than for other HPCs, both for young and mature HPC. As mentioned previously, one reason for this observation may be the type of aggregate in HPC mixes 4 and 7 (granite in HPC 7 and special gravel in both HPC mixes 4 and 7). Those aggregates contained more mica layers than did the aggregates for the resisting HPCs, which was also observed on the ignition losses (Table 2) [4].

Concerning the possible effect of moisture on Poisson's ratio, ν , the internal RH was studied on parallel specimens on each testing occasion. Fig. 6 shows a tendency curve on the effect of RH on ν in mature HPC. ν of mature HPC de-

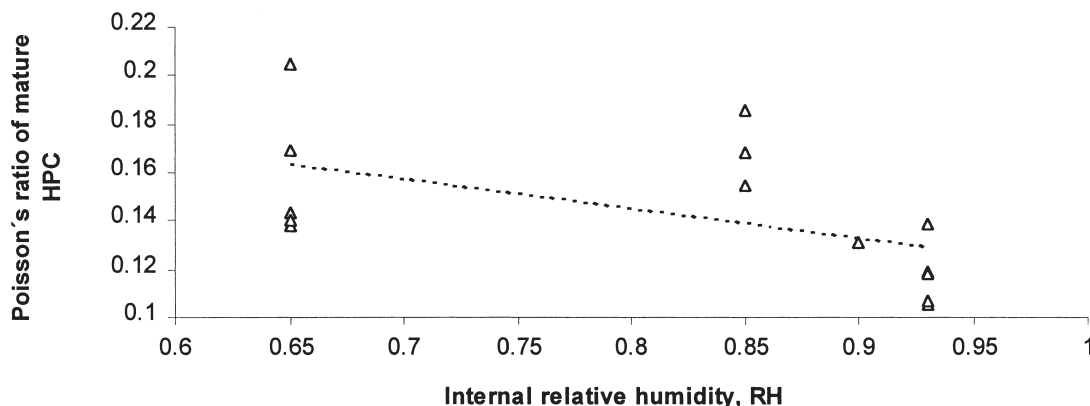


Fig. 6. Tendency curve on the effect of internal RH on Poisson's ratio in mature HPC.

creased with higher RH. The results may be related to the self-desiccation of HPC [10]. However, the significance of the influence of moisture was low. The tendency curves of v were therefore not correlated to RH.

5. Summary and conclusions

An extensive study on Poisson's ratio of HPC subjected to air or sealed curing is reported. Eight qualities of HPC were studied. The concretes contained between 5 and 10% silica fume, and two HPCs additionally contained air-entrainment. Parallel studies of strength and internal RH were carried out. A total of 178 tests were carried out, of which 48 were on young HPC. The tests of mature HPC showed high accuracy. Tests on young HPC exhibited low significance related to the maturity. The tests on young HPC were therefore supplemented by further loading and unloading tests on mature HPC. This study showed a coefficient of variation <0.04 , which was good. The following conclusions were drawn:

- Poisson's ratio, v , was found to be around $v = 0.13$ for mature drying HPC with quartzite.
- Poisson's ratio, v , of a sealed mature HPC with quartzite was found to be about 0.14.
- Poisson's ratio, v , was found to be around $v = 0.16$ for mature HPC with granite.
- Poisson's ratio, v , of young HPC exhibited low significance related to the maturity of HPC.
- At half 28-day strength v became about 0.03 smaller than that of mature HPC.
- Poisson's ratio, v , of sealed young HPC was found to be about 0.03 smaller than that of HPC with air curing.
- The influence of moisture (RH) on Poisson's ratio, v , was not significant.

Acknowledgments

Financial support from BFR (the Swedish Council of Building Research), NUTEK (the Swedish Board of Tech-

nical Development), Cementa, Elkem, Euroc Beton, NCC Bygg, SKANSKA, and Strängbetong is hereby gratefully acknowledged. I am also most grateful to Professor Göran Fagerlund who outlined the present study of HPC and reviewed this article.

References

- [1] J. Brooks, The influence of steel fiber reinforcement on compressive strength and deformation of ultra high strength cement-silica fume mortar matrix, in: I. Holand, E. Sellevold (Eds.), *Proceedings of the 3d Symposium of High-Strength Concrete*, Lillehammer, 1993, pp. 1024–1032.
- [2] J. Brooks, J.P. Hynes, Creep and shrinkage of ultra high-strength silica fume concrete, in: Z.P. Bazant, I. Carol (Eds.), *Proceedings of the 5th International RILEM Symposium on Creep and Shrinkage* (Barcelona), E & FN Spon, London, 1993, pp. 493–498.
- [3] H.H. Bache, *Compact reinforced composite, basic principles*, CBL Report No. 41, Aalborg Portland, Denmark, 1987.
- [4] B. Persson, Quasi-instantaneous and long-term deformations of high-performance concrete with some related properties, Doctoral Thesis, Report TVBM-1016, Lund Institute of Technology, Division of Building Materials, Lund, 1998.
- [5] M. Hassanzadeh, Fracture mechanical properties of high-performance concrete, Report M4:05, Lund Institute of Technology, Division Building Materials, Lund, 1994, pp. 8–13.
- [6] ASTM E 104-85 standard practice for maintaining constant relative humidity by means of aqueous solution, ASTM, Philadelphia, 1985, pp. 33–34, 637.
- [7] B. Persson, Poisson's ratio of high-performance concrete, material properties and design, in: F.H. Wittmann, P. Schwesinger (Eds.), *Proceedings of the 4th Weimar Workshop on High Strength Concrete* held at Hochschule für Architektur und Bauwesen (HAB), Freiburg and Unterengstringen, Weimar, Germany, 1995, pp. 129–143.
- [8] B. Persson, Basic creep of high performance concrete, Report M6:14, Lund Institute of Technology, Division of Building Materials, Lund University, Lund, 1995.
- [9] P.A. Daerga, L. Elfgren, Draghållfasthet hos högpresterande betong, in: *Tensile Strength of High-Performance Concrete*, Bygg & Teknik 7/91, Stockholm, 1991, pp. 25–26 (in Swedish).
- [10] B. Persson, Experimental studies of the effect of silica fume on chemical shrinkage and self-desiccation in Portland cement mortars, in: B. Persson, G. Fagerlund (Eds.), *Proceedings of an International Research Seminar on Self-Desiccation and Its Importance in Concrete* Technology, Division of Building Materials, Lund Institute of Technology, Lund University, Lund, 1997, pp. 116–131.